Numerical Studies on Air-Core Vortex Formation During Draining of Liquids from Tanks[†]

Prateep Basu[1], **Dheeraj Agarwal**[1], **T. John Tharakan**[2], and **A. Salih**[1]

[1]Dept. of Aerospace Engineering, Indian Institute of Space Science & Technology
Trivandrum, India
E-mail: prateepbasu@gmail.com

[2]Flow & Acoustics Division, Liquid Propulsion Systems Centre
Trivandrum, India

The gas-liquid interface dips during the draining of a liquid through a discharge port of a vessel or a tank. The dip develops into a gas-core vortex which subsequently enters the discharge port. This entry can be either gradual or sudden, depending on the intensification of the rotational flow currents during the draining process. The extension of the gas-core into the drain port reduces the flow area and consequently the flow rate. In liquid propellant rocket motors, this phenomenon can have adverse effect on the performance as well as lead to under utilisation of the propellant. In this paper, the authors have tried to find the reason why such an air-core vortex develops in the first place, and the factors that influence its intensification over time, as reported in literature. These investigations have been carried out through simulations done using the commercial ANSYS Fluent code to validate the findings from the CFD results. The simulations are carried out using the volume of fluid (VOF) method, which obtains the volume fraction of each of the fluid throughout the domain and thereby captures the gas-liquid interface motion. Thereafter, the air-core vortex height predictions are validated with results reported in the literature.

* * *

Nomenclature

Q	volume flow rate $[\mathrm{m}^3/\mathrm{s}]$;
d	drain port diameter $[\mathrm{m}]$;
D	vessel diameter $[\mathrm{m}]$;
ρ	density $[\mathrm{kg}/\mathrm{m}^3]$;
H_c	critical height $[\mathrm{m}]$;
μ	dynamic viscosity $[\mathrm{Pa}]$.

[†]Received 07.05.2012

ISSN 1064-2277

Introduction

Of the various dynamic liquid phenomena that may occur in a tank, the rotational motions of the liquid are of special interest. The formation of vortex during draining leads to the reduction in flow rate. This vortex formation occurs because of the torques exerted on the tank through viscous action of the fluid and changes in inertial distribution. Air-entraining vortex behaviour at intakes is an important problem in many situations in hydraulic engineering. Air enters the intake by means of an air entraining free vortex for a certain critical value of the submergence of the intake. The entrained air causes flow reductions, vibrations, structural damage and loss of efficiency in turbines or pumps and in water conveying structures. The motivation for this work stems from the propellant management during draining of propellant from the tank, as the residual propellant in the tank affects launch capability. During the flight of space vehicles and rockets, gas-core vortex develops due to drainage of liquid from the propellant tank to the engines. The rotational flow of the liquid and the consequent extension of the gas-core into the outlet reduce the flow rate of the liquid significantly. Pump fed liquid rocket engines must therefore be cut-off before the pressurant gas enters the pump to prevent over-rotation and possible critical launch failure. Such types of gas-core vortices are observed in day-to-day life such as the bath-tub vortex and kitchen sink vortex.

Lubin and Springer [1] investigated the formation of the air-vortex for the free draining of an initially quiescent column of liquid. Zhou and Graebel [2] performed a numerical study by assuming the potential flow model. They used a cubic-spline nonlinear axisymmetric boundary-integral-method to model the flow. They found for the one-layer-fluid case that when a dip forms, the computed critical heights agree with Lubin and Springer's [1] analytical solution, but only for moderate values of Froude number. An analytical study of this problem was investigated by Stokes et al. [3], who investigated the evolution of a free surface in several different geometric and initial configurations. Ramamurthi and Tharakan [4] carried out experiments with cylindrical tanks, and studied the intensification of this vortex over time. Different configurations and sizes of drain ports have been shown to strongly influence the height of air-core vortex formed during the draining. The rapidly intensifying vortex, quasi-steady vortex and decaying air vortex were identified by Ramamurthi and Tharakan [5]. Recently, Robinson et al. [6] simulated the draining of a cylindrical tank, using computational fluid dynamics and validated the predictions using the experimental work of Lubin and Springer [1]. The versatility of volume of fluid (VOF) approach in modelling such transient draining flows was proven by Robinson et al. [6].

The forces controlling the formation of such gas-vortex during draining from tanks include the gravity force, inertia force and surface tension force. The drain port diameter and vessel dimensions also affect the vortex formation. In this paper, the influence of some of these parameters on the formation and intensification of gas-vortices are studied. The present investigations have been carried out through simulations done using the commercial ANSYS Fluent 13 code.

1. Problem Formulation

The unsteady flow of a viscous liquid through a discharge port located beneath the gas-liquid interface was considered. The CFD simulation involves tracking the gas-liquid interface using the VOF approach. Fig. 1 shows an artist's impression of the axisymmetric draining phenomenon.

Critical height is defined as the height of the liquid column at which the vortex enters the drain port. The flow field for modeling this flow is assumed to be an axisymmetric swirling type, although the actual draining process accompanies a spiral motion on the free surface. To find the swirl

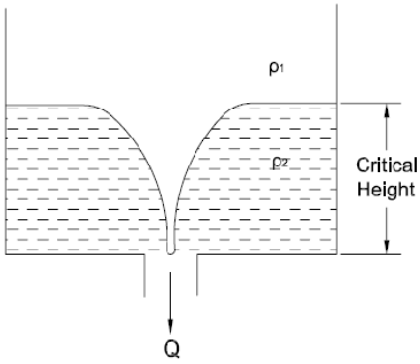

Fig. 1. Schematic of gas-vortex formation during draining.

velocity component in a two-dimensional grid system, the conservation equation for the tangential momentum was applied in addition to the basic axisymmetric governing equation set as follows. The governing equations for this flow are continuity and momentum equations in cylindrical co-ordinates:

$$\frac{1}{r}\frac{\partial}{\partial r}(ru_r) + \frac{\partial u_z}{\partial z} = 0, \tag{1}$$

$$\begin{aligned}
\rho\left(\frac{\partial u_r}{\partial t} + u_r\frac{\partial u_r}{\partial r} + u_z\frac{\partial u_r}{\partial z}\right) &= -\frac{\partial p}{\partial r} + \mu\left[\frac{1}{r}\frac{\partial}{\partial r}\left(r\frac{\partial u_r}{\partial r}\right) + \frac{\partial^2 u_r}{\partial z^2} - \frac{u_r}{r^2}\right] + \rho g_r, \\
\rho\left(\frac{\partial u_z}{\partial t} + u_r\frac{\partial u_z}{\partial r} + u_z\frac{\partial u_z}{\partial z}\right) &= -\frac{\partial p}{\partial z} + \mu\left[\frac{1}{r}\frac{\partial}{\partial r}\left(r\frac{\partial u_z}{\partial r}\right) + \frac{\partial^2 u_z}{\partial z^2}\right] + \rho g_r,
\end{aligned} \tag{2}$$

$$\frac{\partial}{\partial z}(r\rho u_z u_\theta) + \frac{\partial}{\partial r}(r\rho u_r u_\theta) = \frac{\partial}{\partial z}\left(r\mu\frac{\partial u_\theta}{\partial z}\right) + \frac{1}{r}\frac{\partial}{\partial r}\left(r^3\mu\frac{\partial}{\partial r}\left(\frac{u_\theta}{r}\right)\right) - \rho u_\theta u_r. \tag{3}$$

Here, z is the axial component of the coordinate system; r is the radial coordinate component; u_r is the radial velocity component; u_θ is the tangential velocity (swirl) component; u_z is the axial velocity component, ρ is the density of the liquid; μ is its dynamic viscosity. The effects of Earth's rotation and surface tension forces are neglected in the computations. The VOF method tracks the interface between the gas and liquid phases by solving a continuity equation for the volume fraction of gas. The common momentum equation shared between the two phases is as follows:

$$\frac{\partial}{\partial t}(\rho u_i) + u_j\frac{\partial u_i}{\partial x_j} = -\frac{\partial P}{\partial x_i} + \frac{\partial}{\partial x_j}\left(\mu\left(\frac{\partial u_i}{\partial x_j}\right)\right) + \rho g_i, \tag{4}$$

where $\mu = F\mu_1 + (1-F)\mu_2$; $\rho = F\rho_1 + (1-F)\rho_2$; μ is the dynamic viscosity of the cell mix (mix ratio F); ρ is the average density. VOF is computationally more efficient than the Euler-Euler approach because of the common momentum equation. This simplification is valid only when no slip and no interpenetration occur between the phases.

2. Computational Methodology

The commercial CFD code ANSYS FLUENT 13 was used to simulate the transient draining of liquid from a cylindrical vessel. FLUENT uses the finite volume method to break the problem

domain into control volumes in which the transport equations are solved. The VOF multiphase method tracks the interface between the phases by solving a continuity equation for the volume fraction of each fluid throughout the domain. In other words, if the q-th fluid's volume fraction in a cell is denoted by β_q, then the cell contains the interface between the q-th fluid and another fluid for $0 < \beta_q < 1$. This method offers reduced diffusion and a more accurate construction of the interface for a given cell density when compared with more traditional interface tracking schemes ([11]). In order to capture the swirling flow and turbulence effectively, standard $k - \varepsilon$ model for axisymmetric flows was adopted. As the physical situation to be modelled here is transient, the Non-Iterative Time Advancement (NITA) scheme was used, which performs one-iteration per step and thereby significantly speeds up transient simulations. The time step was controlled by Courant number, which was typically chosen between 0.1 and 0.3 depending on the mesh density. The resulting time steps were of the order of 10^{-5} s. Implicit scheme was used for time discretization, and the geometrical reconstruction scheme was used to obtain the face fluxes whenever a cell was completely filled with one phase or another. A pressure based solver was used, as the flow is incompressible. The differencing schemes used were second order upwind for momentum and turbulent kinetic energy. Pressure was discretized using the PRESTO! scheme, which is similar to the staggered-grid schemes used with structured meshes. The PISO algorithm was used for the pressure-velocity coupling as it is more efficient than SIMPLE and SIMPLEC algorithms, since it performs two additional corrections: momentum correction and mesh skewness correction.

2.1. Computational mesh. Two dimensional structured grids were generated to represent the different possible test geometries. The number of cells were varied from 5000 to 80000 typically, for the meshes with configuration $d/D = 2/25$, so as to achieve mesh independent solutions. For this particular configuration, the acceptable mesh density is for the one with 46600 cells as it showed a change less than 1% in the outflow mass flow rate. Structured grids were used since the geometry is not complicated and gradients were almost absent, except near the drain port. Fig. 2 shows some typical meshes used for simulations.

2.2. Boundary conditions. A large gas to liquid volume ratio was assumed so that the gas pressure above the liquid could be considered as constant. The boundary conditions for modelling the flow are given in Table 1.

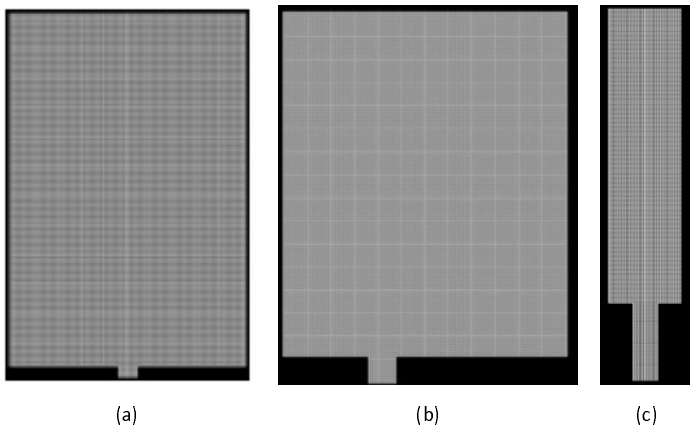

Fig. 2. Calculation domains and meshes:
a) $d/D = 1/8$; b) $e = 0.5$; c) $d/D = 1/3$.

Table 1.
Boundary conditions

Wall	Viscous/No Slip ($u_z, u_r = 0$), Inviscid/Slip ($u_z = U, u_r = 0$)
Inlet	Pressure Inlet (Gauge pressure $= 0$)
Outlet	Pressure Outlet (Gauge pressure $= 0$)
Interface	Stress free, Wall adhesion effects (contact angle: 90°)

Table 2.
Results of CFD analysis

Run	Specific gravity	Liquid	Start depth to orifice radius ratio	Orifice radius to critical height ratio	Critical discharge
1.1	1	water	7.50	0.429	376.184
1.2	—	—	9.33	0.450	388.560
2.1	0.78	kerosene	10.0	0.360	234.270
3.1	0.79	ethyl alcohol	7.50	0.454	226.367
4.1	0.61	liquid NH_3	10.0	0.225	180.991
4.2	—	—	20.0	0.280	187.590
5.1	0.855	turpentine	15.0	0.520	162.245

3. Results and Discussion

In the simulation of liquid draining from a vessel, the VOF model has been shown to give a good account of draining characteristics in a qualitative and quantitative sense, as previously shown by Robinson et al. [6]. The dip inception is detected by the first inflection in the iso-contours of volume fraction at the interface as indicated in Fig. 3. The critical heights obtained from the CFD simulations are found to be higher than that reported by Lubin and Springer [1] or Zhou and Graebel [2]. This is because the interface deforms in a very short period of time and the CFD method allows this dip to be captured earlier, as a result giving slightly higher critical heights for the same set of experimental conditions. The lower and upper fluids are taken as water and air respectively. Hence, the interface is neutrally stable.

3.1. Effect of critical discharge. Draining was carried out at fixed Froude numbers, in a way similar to that of the boundary integral method (BIM) work done by Zhou and Graebel [2], keeping

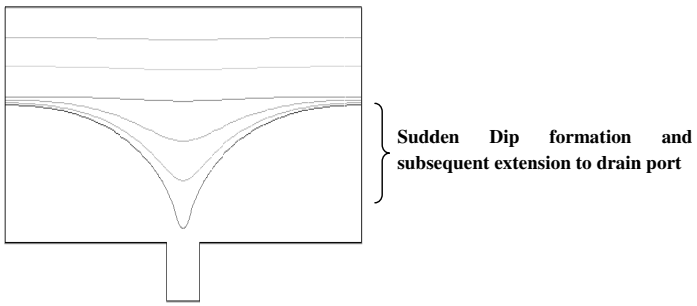

Fig. 3. Time development of free surface.

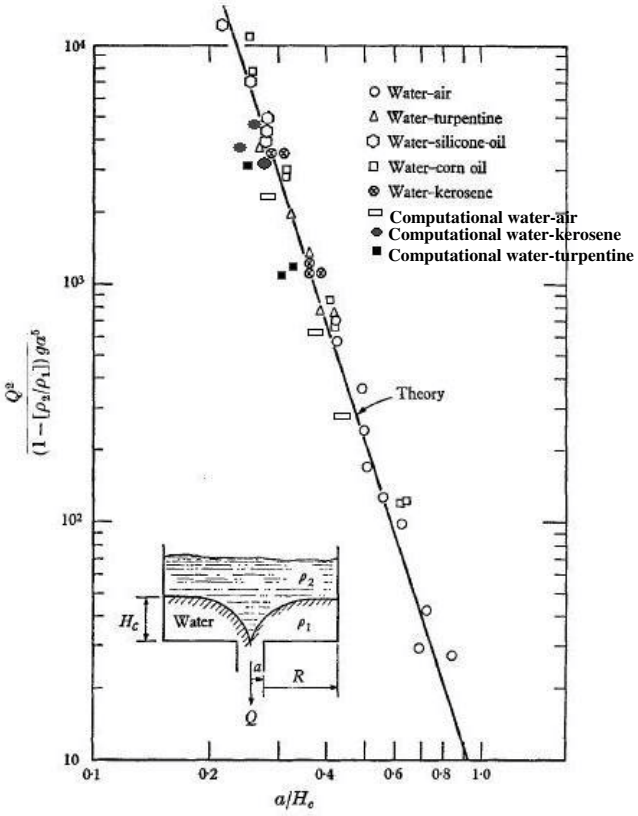

Fig. 4. Comparison between experimental data of Lubin and Springer [1] and the present computational results.

the flow rate constant. This draining process with fixed Froude Number is analogous to putting a pump on the outlet pipe of the experimental setup of Lubin and Springer [1]. The results of the simulations for radius aspect ratio (d/D) of 0.25 are as tabulated in Table 2. The last column in Table 2 indicates the non-dimensionalized critical discharge given by $Q^* = Q_2/[(1 - \rho_2/\rho_1)^* g d^5]$. The penultimate column provides values for the ratio of orifice radius to critical height, as defined in the original work of Lubin and Springer [1]. The first column simply indicates the case number that is used. Simulation series 1–5 were carried out to populate the list of cases needed to replicate the work of Lubin and Springer [1] and then gauge the CFD predictive capabilities versus the previous experimental and analytical work. Equation for Q^* represents the regression line computed by Lubin and Springer [1], which is also shown as a solid line in Fig. 4. The values tabulated below for critical height are obtained by keeping the initial height and drain port radius constant, and varying the bottom liquid.

The initial height is found to affect the critical height, which is in accordance with the work of Robinson et al. [6], who also predicted that large initial heights affect the critical vortex height. But it is difficult to arrive at the reason for the slight increment of critical height for very high initial heights from the results of the present investigations. No initial rotation was imparted to the liquid during the course of simulation.

3.2. Effect of Froude number. The simulations are repeated by varying the drain port diameter, and there by the Froude number. Free surface flows such as these are characterized by Froude

number, which is basically the ratio of inertia forces to body forces. Large Froude numbers correspond to large drain velocities and consequently larger values of the liquid draw down acceleration. The height of the gas-vortex is more compared to the prediction of Lubin and Springer [1] due to the unsteady term du/dt considered (in the equations for computation) in the present simulations. This difference increases as the Froude number is increased. The variation of critical Height with Froude number is depicted in Fig. 5. For small values of Froude number, the draw-down due to inertia force is lower in comparison with gravitational force. This gives rise to lower radial pressure gradient in the tank. Two different flow phenomena are thus possible depending on flow parameters i. e.,

(i) a dip;

(ii) a reverse jet as shown in Fig. 6.

A more concentrated draw-down force overcomes the squeezing of the near centre surface points by the off-centre surface points, and a pulling-down of the centre of the free surface. Thus a sufficiently

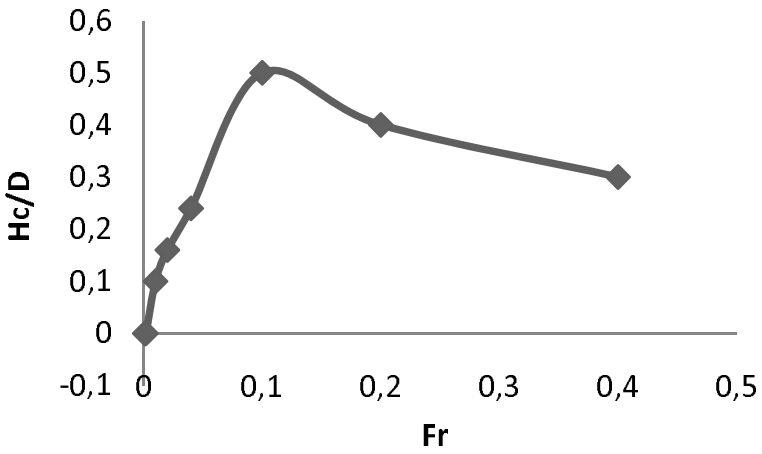

Fig. 5. Effect of Froude number on critical height.

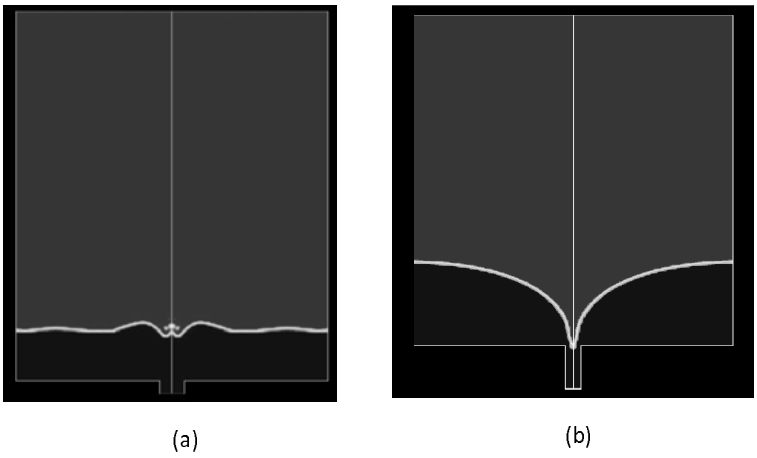

Fig. 6. Surface effects: a) reverse jet; b) late sudden dip.

small d gives rise to a profound dip as shown in Fig. 6b. If d is not sufficiently small, the squeezing together of the near-centre surface points decelerates the centre. Consequently, it generates a reverse jet as shown in Fig. 6a. Such a reverse jet is also reported by Zhou and Graebel [2] in their original work.

3.3. Effect of pressure on draining. It is seen from Fig. 7 that the pressure far away from the centreline is nearly hydrostatic with almost constant pressure gradient, and there is a large radial pressure gradient in the vicinity of the discharge port. In the absence of a dip, gas-liquid interface and the liquid beneath it are of zero pressure gradient. The free surface will be the zero pressure line, along with another one inside the flow regime at early times when dip is not formed. Initially, the patterns of constant pressure lines are similar for both cases. The merging of the two zero pressure lines is the necessary condition for the formation of a dip, as proposed by Zhou and Graebel [2]. However, there are substantial differences in the pressure distribution at a later stage which result in the different phenomena. The pressure at the axis of the tank is less than that of its neighbourhood. This leads to the draws-down of the centre of the free surface, there by forming a dip. The total pressure along the interface varies thereafter, due to the presence of radial pressure gradient. The net pressure force does not pass through the center of mass, and the resulting torque changes the vorticity and circulation. It generates a positive circulation, which causes the denser fluid to slump under the lighter one until eventually an equilibrium is reached with the lighter fluid layered on top of the denser fluid. Hence, the drainage of a liquid from an axisymmetrically placed discharge port beneath the liquid is a baroclinic process, because of the interaction of the pressure and density fields in a stratified fluid.

3.4. Effect of geometrical and flow parameters. The variation of critical height with diameter ratio (d/D) is given in Fig. 8. The dip is markedly formed for a certain range of d/D values only. For very small or very large values of d/D, the liquid simply drains out like a potential sink type flow. Hence, there exists a critical range of flow rates for which deformation of the free surface happens. For the current set of simulations, the range of d/D for which the dip was formed

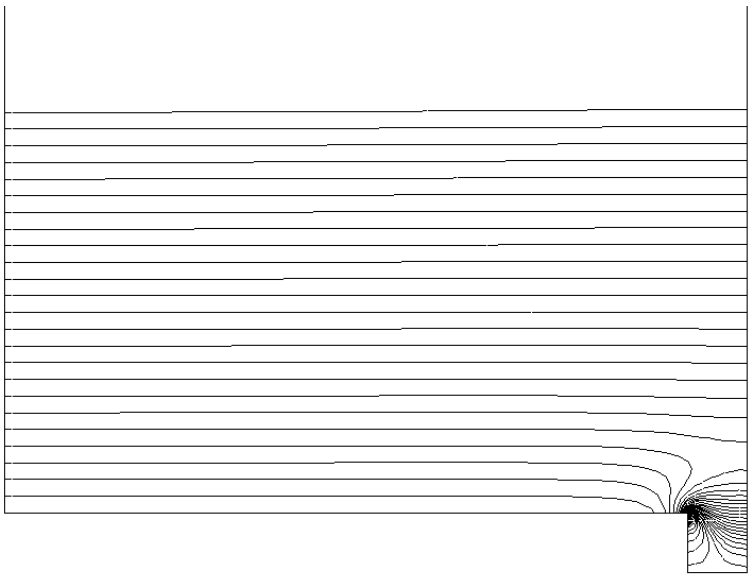

Fig. 7. Contours of static pressure after the dip is formed.

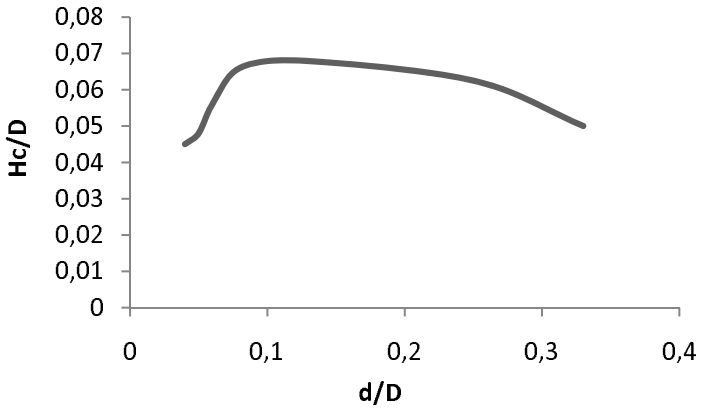

Fig. 8. Variation of critical height with diameter aspect ratio.

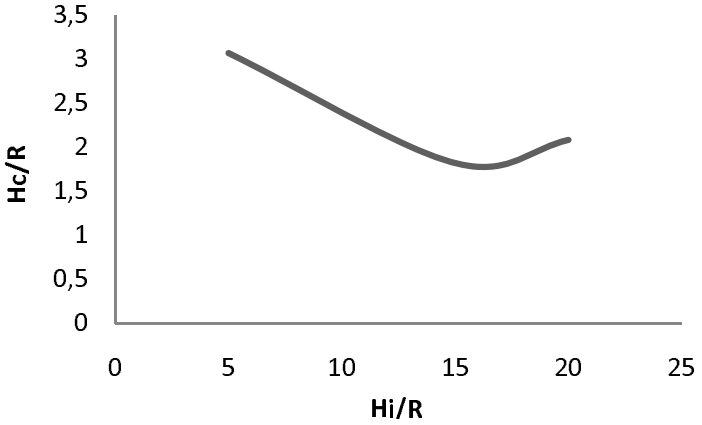

Fig. 9. Effect of critical height with initial height.

was found to be between the values $0.04 - 0.33$. This corresponds to moderately high values of Froude number, which is in agreement with the results of subsection 3.2. The critical height is also influenced by the flow parameters and liquid properties such as initial height of the liquid column (Fig. 9), acceleration due to gravity (Fig. 10), density (Fig. 11), suction pressure (Fig. 12) and initial swirl velocity. This may be because the smoothening of the free surface is difficult when it is under strain due to draining, especially under adverse physical conditions as shown by the aforementioned plots. For liquids having viscosity close to that of water, it is found to have negligible effect on the critical air-vortex height. The role of viscosity of a liquid is to diffuse the already present vorticity in the liquid. This is in agreement with the experimental findings of Ramamurthi and Tharakan [5]. But for highly viscous liquids like honey, the same may not hold true.

3.5. Formation and intensification of air-core vortex. The vortex strength is defined as the difference in the tangential velocities across an interface. The interfacial vortex strength for a large stratification is higher than that for a small stratification; with the maximum vortex strength appearing at the trough of the interface, which in this case is at the drain port, as shown in Fig. 13. The intensification region is primarily characterized by amplification of rotation due to convective evolution of vorticity. A discontinuity in tangential velocity at the gas-liquid interface can lead

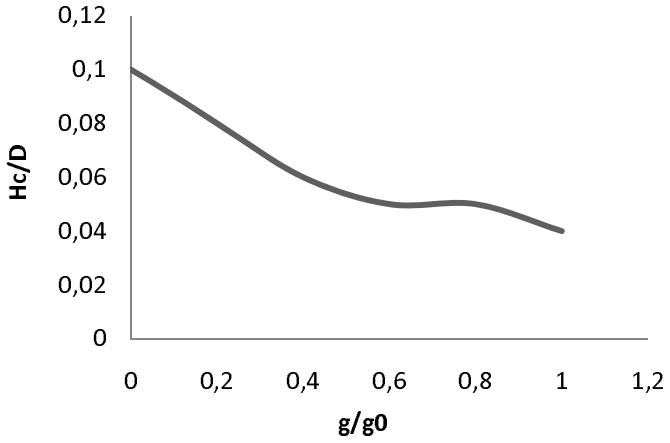

Fig. 10. Effect of critical height with gravity.

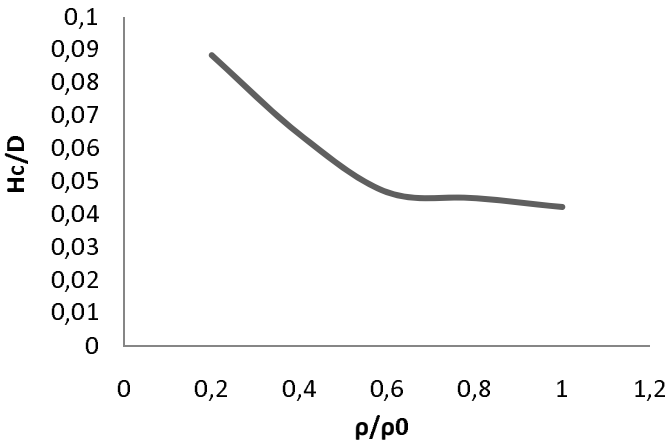

Fig. 11. Effect of critical height with density.

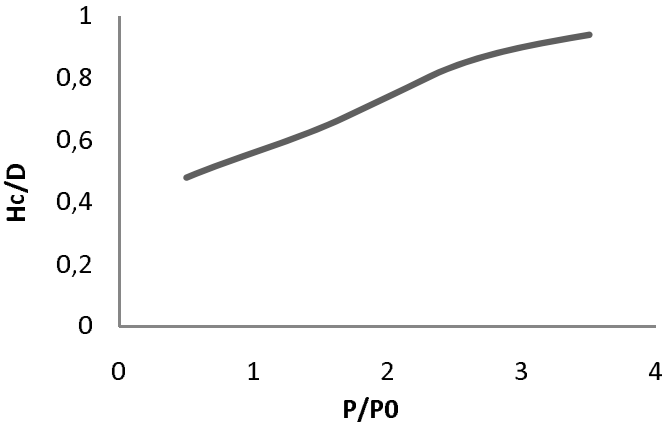

Fig. 12. Effect of critical height with suction pressure.

to the formation of a vortex dipole. The vortex dipoles and also their combinations (e. g. vortex quadrupoles) are the universal products of any irregular forcing in two-dimensional flows. In the present case, it is the density stratification that produces such a dipole. The presence of a dipole in the present case can be substantiated from the radial velocity contour plot, as shown Fig. 14, where the radial velocities have negative value near the drain port. The swirling liquid near the drain-port leads to the formation of a small low pressure zone, which results into the deformation of the free surface above it. The intensification of the depression (dip) formed at the surface of the liquid, into a strong air-core vortex had been shown by Ramamurthi and Tharakan [5] through their experiments, and reported by Zhou and Graebel [2], who also observed the intensification of air-core vortices with almost sudden ingestion of the upper fluid. The same has been found through CFD simulations. The

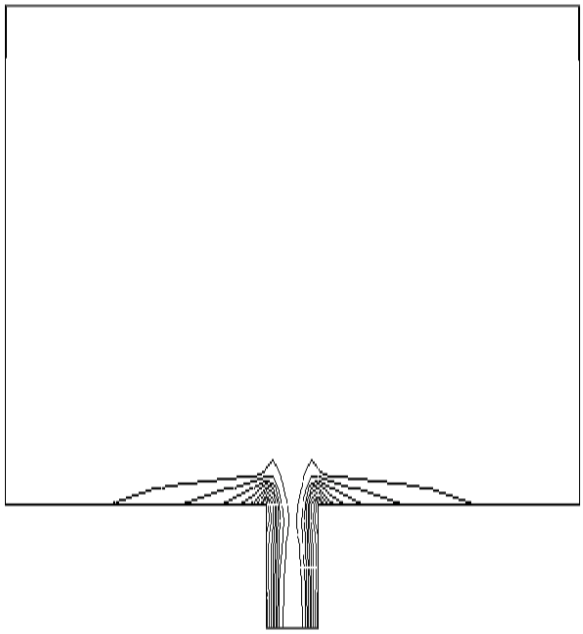

Fig. 13. Vorticity plot showing the dipole at the drain port inlet.

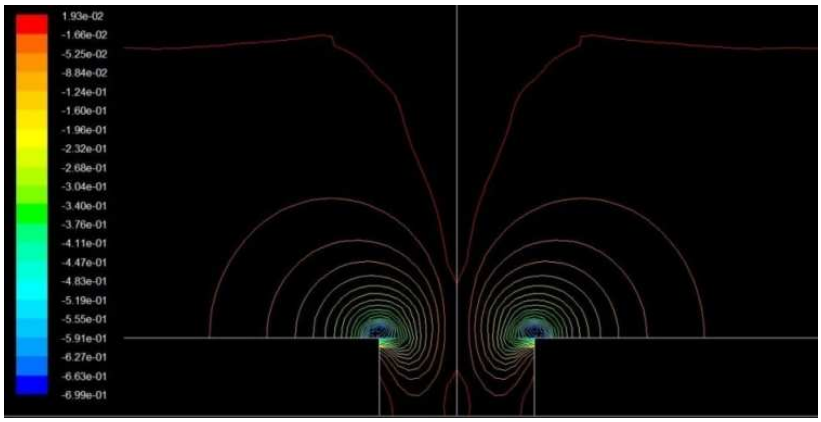

Fig. 14. Contours of radial velocity at the drain outlet.

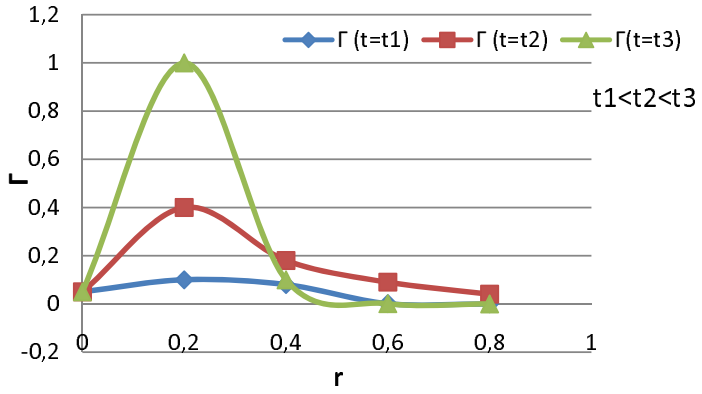

Fig. 15. Time development of vortex strength along the radius of the tank.

interfacial vortex strength for the two layer stratified fluid increases with time, mainly near the axis of the tank, as shown in Fig. 15.

3.6. Draining through eccentric discharge ports. Gowda et al. [7] showed that vortexing can be reduced by using tanks of square and rectangular cross sections. Another way of reducing gas-vortexing can be by using eccentric discharge ports. Experiments of Gowda et al. [7] and Ramamurthi and Tharakan [4] showed that on increasing the eccentricity, the values of critical height decreased. The same was observed on carrying out simulations with eccentric drain ports. The dip appeared relatively later, and the time taken for draining was also higher by approximately 12%. The probable physical explanation for the prevention of vortexing with eccentricity of the drain port is that drain ports with increasing eccentricity are located in regions of relatively higher pressures; hence the dip cannot extend to the port as effectively as in case of axisymmetric port, and thus gas-vortexing is suppressed. The growth of dip along the axis of symmetry of the vessel is easier because of the lower pressure acting on the centreline of the tank. The asymmetry in the vorticity field combined with the effect of pressure lead to lower critical heights for eccentric drain ports.

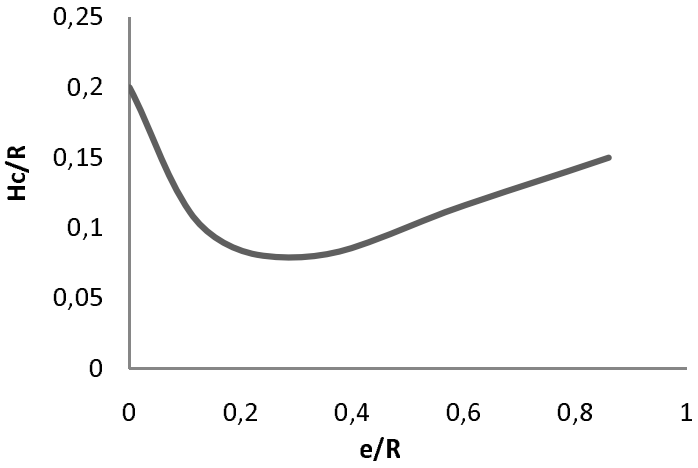

Fig. 16. Effect of eccentricity on critical height.

The expected trend is obtained in Fig. 16, which is different from the prediction of Gowda et al. [7]. This might be due to the presence of initial rotational velocity in the experiments by Gowda et al. [7]. Eccentricity is observed to reduce the air-core vortex critical height at first, but it ceases to have any effect for $e > 0.6$. It is to be noted that differences in asymmetry of the flow field cannot be observed through naked eye, as the variations are very small. Visualization techniques can be used in future to study this phenomenon in more detail.

3.7. Draining under microgravity conditions. Liquid acquisition in microgravity conditions is a very difficult task, majorly because of the reorientation of the liquid in the container under the action of even small forces. A marked dip was reported to occur (by Abramson [8]) in the interface as the liquid is forced out by a pressurizing gas and the same trend is observed in simulations as shown in Fig. 17. Due to the absence of gravity, the only smoothening force for the interface is the surface tension. Hence, the surface tension model adopted for simulating the draining will affect the shape of the interface. Surface tension is approximated within FLUENT by the continuum surface force (CSF) model of Brackbill et al. [9]. Wall adhesion is used in FLUENT in conjunction with the surface tension approximation. This model adjusts the curvature at liquid solid interfaces to take contact angles into account. Blow through occurs if the draining velocity is too large. It is evident that considerable precaution is necessary in the design of a liquid-venting system for zero-g operation or else large amounts of liquid may be retained, if adequate precautions are not taken. The profiles shown in the schematic and the CFD simulation differs at the boundaries, because of the different liquid chosen and the contact angles made by them with the wall. A relatively different phenomenon happens if the drain rates are higher. The free surface shoots up like a fountain, resulting in negative liquid acquisition at the drain outlet. These geysers are usually observed at reverse gravity acceleration greater than certain critical values of acceleration during the course of liquid reorientation.

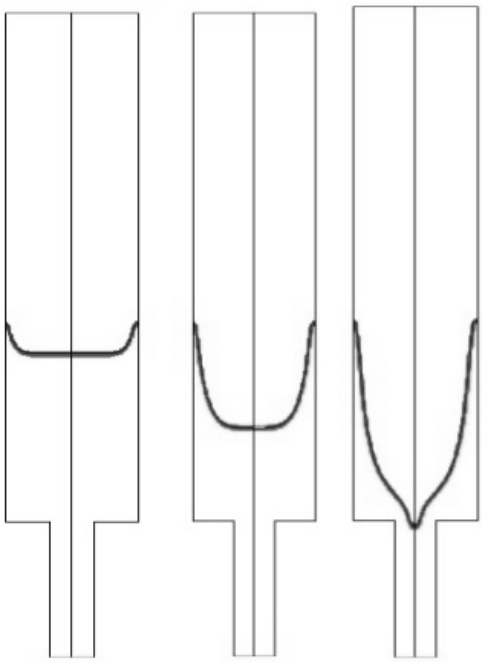

Fig. 17. Interface profile on draining in microgravity.

Conclusions

Numerical investigations on vortex formation during draining from a tank have been successfully carried out to have an understanding of the phenomenon, in terms of physical and geometrical parameters. The following conclusions are made:

- The simulations provided a probable theoretical explanation for the formation and intensification of a gas-core vortex, while draining axisymmetrically from tanks.
- The range of Froude numbers for which a dip, and subsequently a vortex is formed, is found through these CFD simulations.
- The effect of diameter aspect ratio (d/D) and discharge on critical height of the liquid is investigated. It is found that for very low or very high d/D values, vortex is not formed.
- It is shown that such free drain vortices are formed because of the action of a vortex dipole, present at the drain port.
- Baroclinicity in the flow due to non parallel pressure and density field may be a factor for intensifying the vortex.
- The results obtained through CFD are in good agreement with previously reported experimental and numerical observations.

The results obtained from these simulations can act as inputs for tank outlet design, for dip-free draining from propellant tanks of rockets, pumps and intake systems in hydraulics engineering. From the perspective of liquid propellant management during flight, the location and value of minimum pressure can be determined using the results of this study, which might ensure cavitation free flow inside the pump by maintaining a higher vapour pressure of the propellant than this minimum pressure. The impulsively started draining process, with the presence of initial swirling, is in agreement with the conservation of angular momentum principle. The accuracy of the predictions could be improved with increase in computing power. In future, theoretical work can be taken up to find out the criticality condition for such air-core vortex to form in terms of geometrical and flow parameters, and the stability of such vortices can be analysed using mathematical tools.

REFERENCES

1. Lubin, B. T. and Springer, G. S., The Formation of a Dip on the Surface of a Liquid Draining From a Tank, *J. Fluid Mech.*, 1967, **29**, pp. 385–390.
2. Zhou, Q. N. and Graebel, W. P., Axisymmetric Draining of a Cylindrical Tank with a Free Surface, *J. Fluid Mech.*, 1980, **221**, pp. 511–532.
3. Stokes, T. E., Hocking, G. C., Forbes, L. K., Unsteady Free Surface Flow Induced by a Line Sink in a Fluid of Finite Depth, *Comput. Liquids*, 2008, **37**, No. 3, pp. 236–249.
4. Ramamurthi, K. and Tharakan, T. J., A Study of Vortex Formation during Discharge of Liquids from Cylindrical Containers, *J. Aero. Soc. Ind.*, 1992, **44**, No. 1, pp. 59–66.
5. Ramamurthi, K. and Tharakan, T. J., Intensification of a Vortex during Draining, *Can. J. Chem. Eng.*, 1995, **73**, pp. 292–299.
6. Robinson, A., Morvan, H., and Eastwick, C., Computational Investigations into Draining in an Axisymmetric Vessel, *J. Fluids Eng.*, 2010, **132**, No. 12, pp. 121104(1–7).

7. Sohn, C. H., Gowda, B. H. L., and Ju, M. G., Eccentric Drain Port to Prevent Vortexing During Draining from Cylindrical Tanks, *J. Spacecrafts and Rockets*, 2008, **45**, No. 3, pp. 638–640.
8. Norman Abramson, H., *Some Studies in Liquid Rotation and Vortexing in Rocket Propellant Tanks*, NASA TN D-1212.
9. Brackbill, J. U., Kothe, D. B., and Zemach, C., A Continuum Method for Modelling Surface Tension, *J. Comput. Phys.*, 1992, **100**, No. 2, pp. 335–354.
10. Batchelor, G. K., *An Introduction to Fluid Dynamics*, Cambridge Univ. Press, Cambridge, UK, 1970.
11. Fluent, Fluent 13 User's Guide, 2006.

□◆◆◆□